# Supporting Information for

# Actuated Dielectric-Lossy Screen for Dynamically Suppressing Electromagnetic Interference

Andrew D. M. Charles[ab]*, Andrew N. Rider[a], Sonya A. Brown[b] and Chun H. Wang[b]

[a] Defence Science and Technology Group, 506 Lorimer Street, Fisherman's Bend, VIC, Australia, 3207

[b] University of New South Wales, School of Mechanical and Manufacturing Engineering, Sydney, NSW, Australia, 2052.

*Corresponding author at Defence Science and Technology Group, 506 Lorimer Street, Fisherman's Bend, VIC, Australia, 3207 (Andrew D. M. Charles), E: andrew.charles@dst.defence.gov.au, P: +61 3 9626 7263, F: +61 3 9626 7174

## S1.    Analytical Solution for Layered Absorber

The reflection coefficient (R) of the aDLS can be estimated using the following analytical solution for a layered absorber backed by a perfect electrical conductor (PEC),

$$R = \frac{r_{01} + R_2 \exp(-2i\delta_1)}{1 + r_{01}R_2 \exp(-2i\delta_1)} \tag{S1}$$

where $R_2$ is the reflection coefficient from the second layer,

$$R_2 = \frac{r_{12} + R_3 \exp(-2i\delta_2)}{1 + r_{12}R_3 \exp(-2i\delta_2)} \tag{S2}$$

and $R_3$ is the reflection coefficient of the third layer,

$$R_3 = \frac{r_{23} + r_{34} \exp(-2i\delta_3)}{1 + r_{23}r_{34} \exp(-2i\delta_3)} \tag{S3}$$

whilst $r_{01}$, $r_{12}$, $r_{23}$, and $r_{34}$ are the Fresnel reflection coefficients from the respective air-MPC, MPC-QFRP, QFRP-air and air-PEC interfaces,

$$r_{01} = \frac{\sqrt{\frac{\mu_1}{\varepsilon_1}}-1}{\sqrt{\frac{\mu_1}{\varepsilon_1}}+1}, \; r_{12} = \frac{\sqrt{\frac{\mu_2}{\varepsilon_2}}-\sqrt{\frac{\mu_1}{\varepsilon_1}}}{\sqrt{\frac{\mu_2}{\varepsilon_2}}+\sqrt{\frac{\mu_1}{\varepsilon_1}}}, r_{23} = \frac{\sqrt{\frac{\mu_3}{\varepsilon_3}}-\sqrt{\frac{\mu_2}{\varepsilon_2}}}{\sqrt{\frac{\mu_3}{\varepsilon_3}}+\sqrt{\frac{\mu_2}{\varepsilon_2}}}, r_{34} = \frac{\sqrt{\frac{\mu_4}{4}}-\sqrt{\frac{\mu_3}{\varepsilon_3}}}{\sqrt{\frac{\mu_4}{\varepsilon_4}}+\sqrt{\frac{\mu_3}{\varepsilon_3}}}$$

and $\delta_i = (\frac{2\pi}{\lambda})d_i\sqrt{\varepsilon_i\mu_i}$, where $d_i$, $\varepsilon_i$ and $\mu_i$ are the thickness, permittivity and permeability of layer $i$. As the ground plane is considered a perfect electric conductor (PEC), we have $r_{34} = 0$.

Using this analytical approach, the variation in reflection coefficient as a function of frequency and layer 1 thickness ($d_1$) for various layer 3 thicknesses ($d_3$) and a fixed layer 2 thickness ($d_2$ = 0.6 mm) have been computed; the results are presented in Figure S1. In this instance, layer 1 was modelled using the optimized and measured material properties (detailed in the manuscript as CNT content of 1.5 vol. % and CIP content of 5.9 vol. %), layer 2 was modelled to represent the QFRP, with $\varepsilon_r$ = 3-0.08i and $\mu_r$ = 1 and layer 3 was set to free-space properties (i.e. $\varepsilon_r$ = 1, $\mu_r$ = 1).
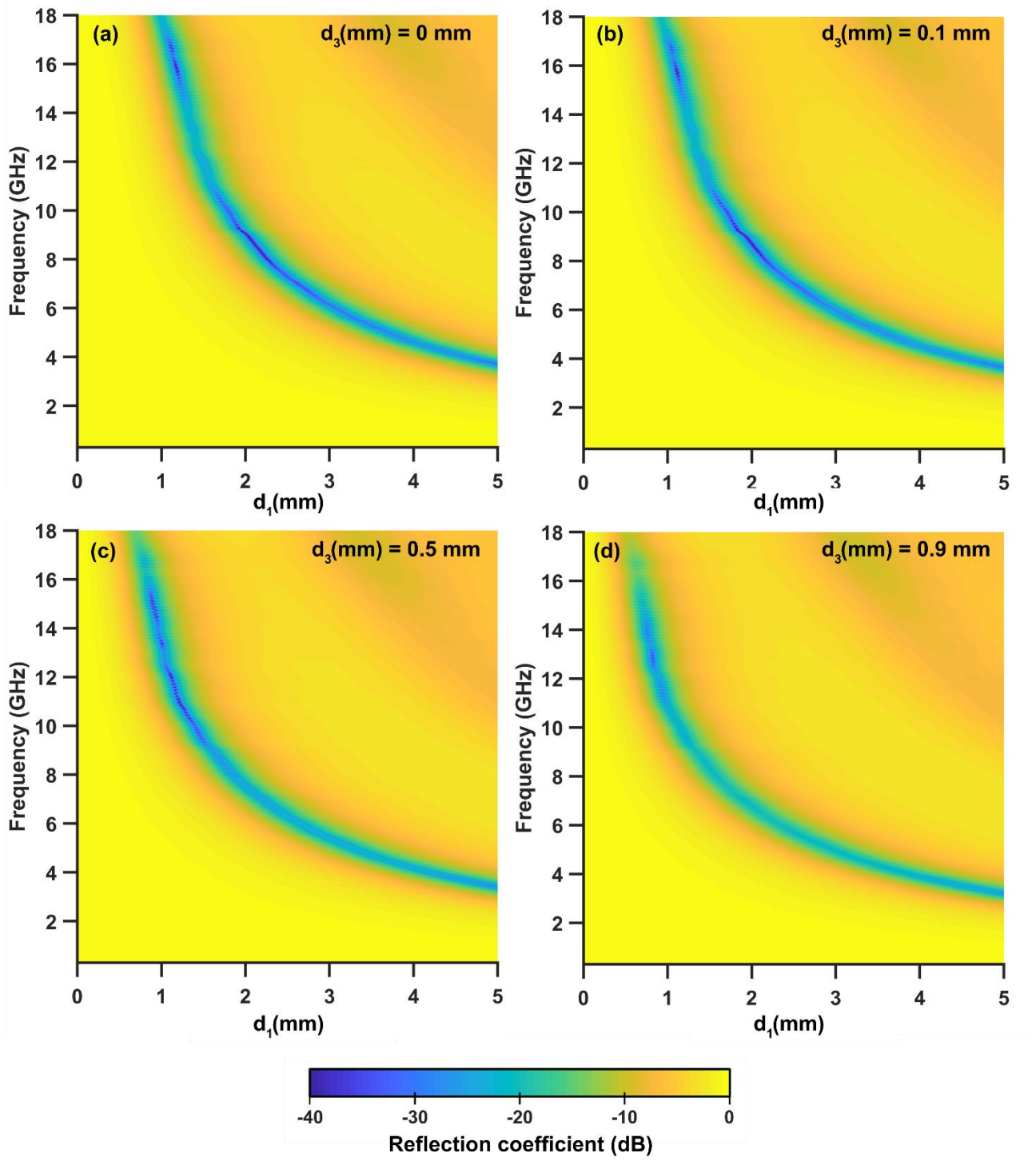
**Figure S1**. Calculated reflection coefficient as a function of frequency and $d_1$ thickness for different $d_3$ thicknesses with $d_2 = 0.6$ mm, $\varepsilon_1$ and $\mu_1$ measured for CNT content of 1.5 vol. % and CIP content of 5.9 vol. %, $\varepsilon_2 = 3\text{-}0.08i$, $\mu_2 = 1$, $\varepsilon_3 = 1$, $\mu_3 = 1$: (a) $d_3 = 0$ mm, (b) $d_3 = 0.1$ mm, (c) $d_3 = 0.5$ mm and (d) $d_3 = 0.9$ mm.

## S2.    Electrical Percolation Measurements

The electrical percolation was measured in CNT and CIP filled epoxy using two different techniques. For CNT filled epoxy, due to the higher intrinsic conductivities expected (typically $10^5$ - $10^7$ S/m[1]), a four-point-probe was used (T2001A3, Ossila, UK), with $\Omega/\square$ values reported. For the CIP filled epoxy, due to the higher expected resistivities, a custom measurement cell was utilized[2], with volumetric resistivity ($\Omega$.m) reported. Results for the respective CNT/epoxy and CIP/epoxy samples as a function of volume concentration are shown in Figure S2. Sigmoidal fits to the experimental data are shown in each image, suggesting electrical percolation occurs at approximately 3.3 vol. % and 11.9 vol. % for CNT and CIP loaded epoxy respectively.
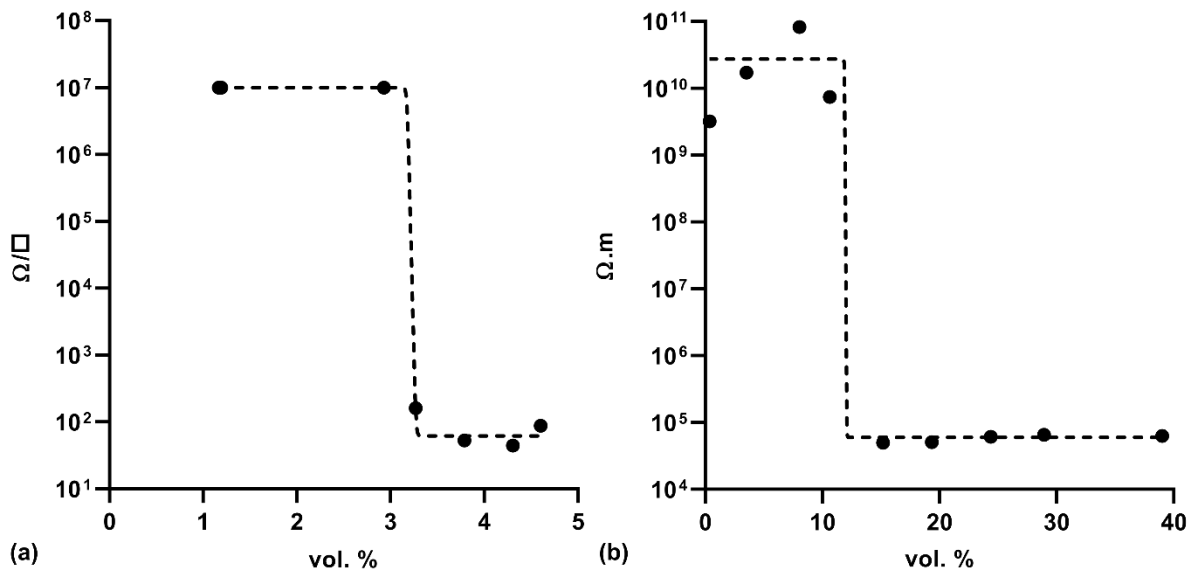


**Figure S2.** electrical percolation results for (a) CNT/epoxy composites as a function of CNT volumetric loading and (b) CIP/epoxy composites as a function of CIP volumetric loading.

## S3.    Optimization Algorithm

Given the measured magneto-polymer composite (MPC) properties as a function of CNT and CIP volumetric loading, this data was utilized in an optimization regime to determine dielectric lossy sheet (DLS) thicknesses which minimizes reflection at a fixed frequency. To achieve this, MATLAB's global optimization toolbox was utilized, with the in-built genetic algorithm implemented. In this instance, the objective function for minimization was the DLS reflection coefficient at a 9 GHz, implemented via the analytical process detailed in Section 2 of the manuscript and Section S1 previously. Optimization variables were the MPC thickness ($d_1$) and spacer thickness ($d_3$) as detailed

in Fig. 1(a) of the manuscript, with these both constrained to within 0-10 mm. A population size of 500 was established, with the maximum number of generations also set to 500.

## S4.  Epoxy Degree of Conversion

The degree of conversion for the base epoxy system was established using Differential Scanning Calorimetry (DSC). An uncured sample of the epoxy (combined parts A and B) was heated twice from -10 to 300°C at a rate of 10°C/min. The degree of conversion was calculated using the methodology detailed by Ryu et al.[3], with the measured heat flow and calculated degree of conversion results presented in Figure S3.
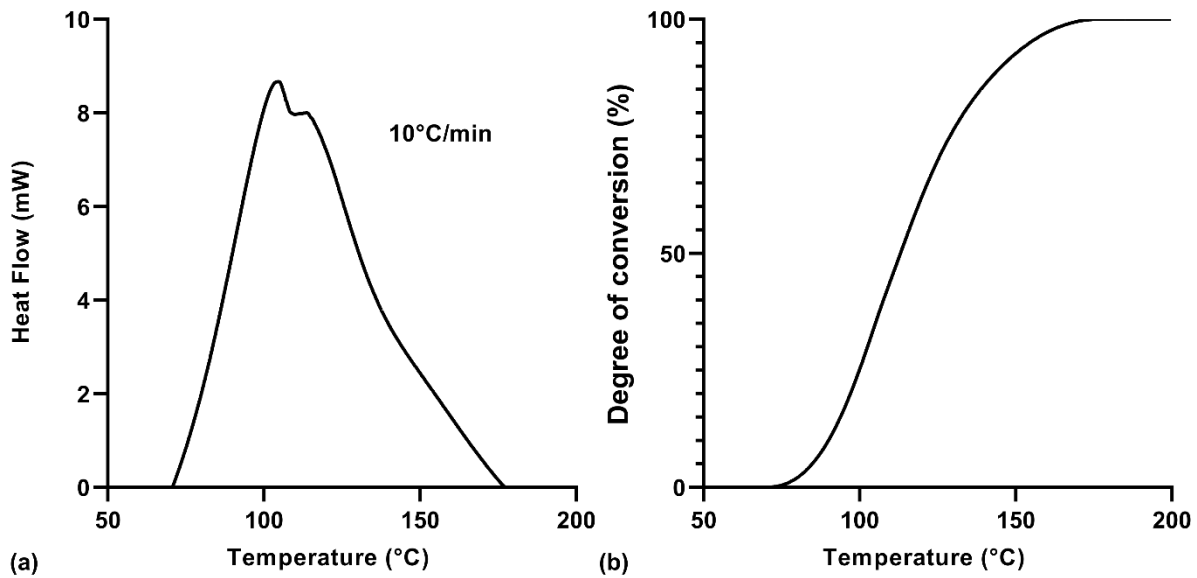


**Figure S3**. (a) Heat flow and (b) degree of conversion for the LY3600 epoxy resin system.

## S5.  Manufacturing Details

A slight curvature was observed in the actuated dielectric lossy sheet (aDLS) structure, attributed to poor release between the MPC and QFRP layers, achieved by the fiberglass reinforced PTFE film. This curvature is shown in Figure S4, with close-up views of the PTFE film layer shown in Figure S5. As can be seen in Figure S5, good connection is observed between MPC, QFRP and the fiberglass reinforced PTFE film interlayer, suggesting reasonable adhesion between these layers, accounting for the curvature observed.
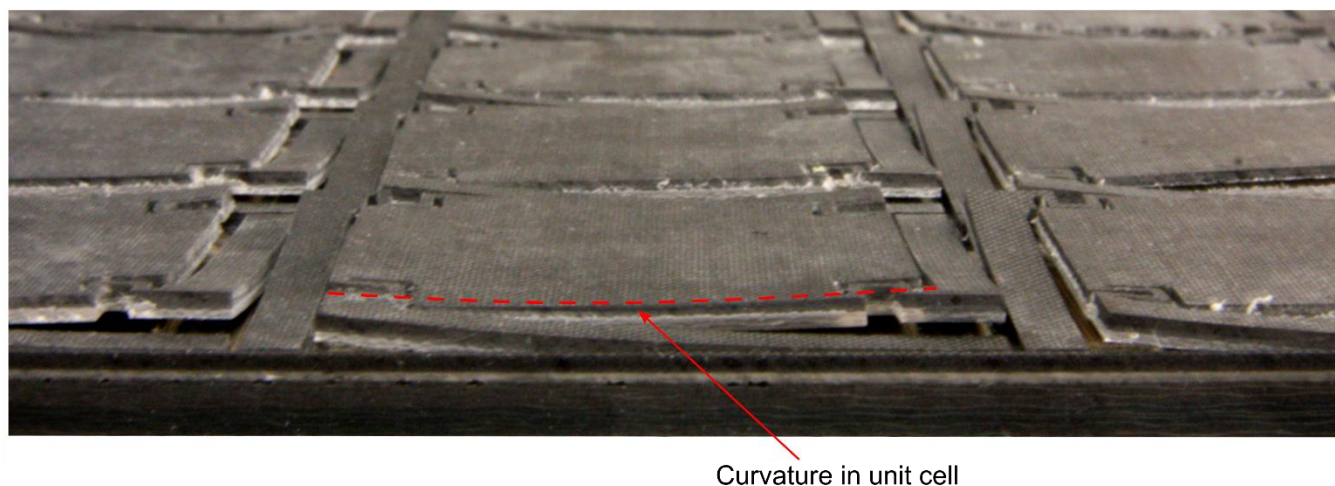
Curvature in unit cell

**Figure S4**. Side view of manufactured aDLS structure showing a slight curvature observed in the unit cell surface.



(a)

fiberglass
reinforced PTFE

End of fiberglass
reinforced PTFE

MPC

QFRP

0.5 mm
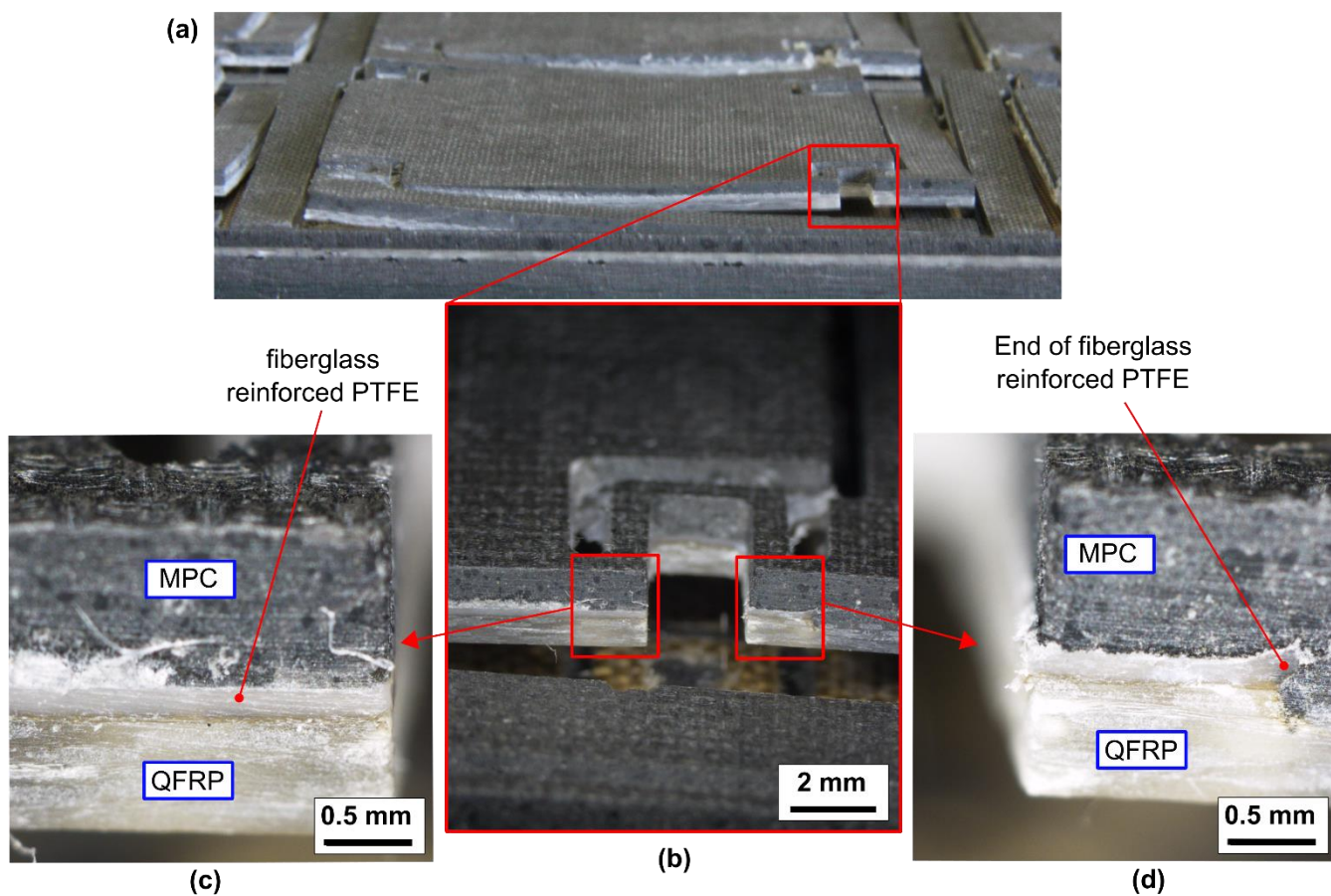
MPC

QFRP

0.5 mm

2 mm

(c)

(b)

(d)

**Figure S5**. Magnified image of serpentine structure showing the fiberglass reinforced PTFE film layer. (a) Side view of unit cell, (b) close-up view of serpentine structure with further call outs to (c) and (d) showing the existence of the fiberglass reinforced PTFE film between MPC and QFRP layers in this region.

## S6.    Multi-Physics Modelling

Figure S6 shows the multi-physics model implemented to investigate the deflection response of the aDLS as a function of temperature. As discussed in the manuscript, two models were implemented, one in which the MPC and QFRP layers were not connected in the central region of the aDLS structure (Figure S6 (b)), and the other in which a perfect connection was assumed (Figure S6 (c)).
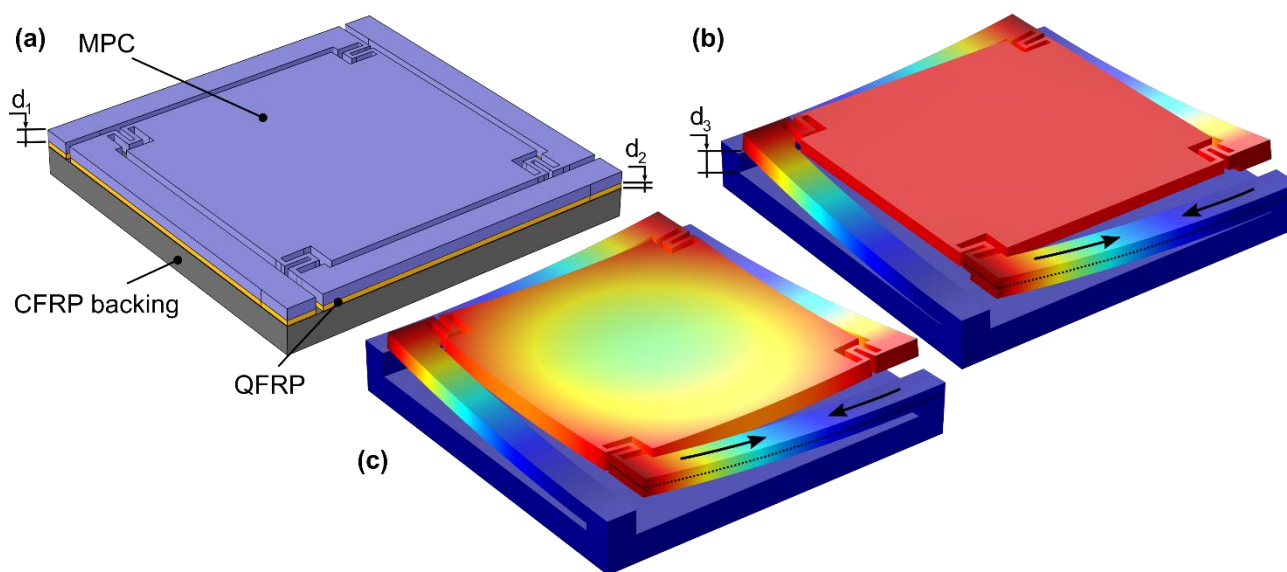


**Figure S6**. Multi-physics model of a single aDLS unit showing (a) the undeformed geometry with relevant materials, (b) the deformed geometry with no MPC-QFRP connection and (c) and the deformed geometry with MPC-QFRP connection. Arrows in (b) and (c) indicate the MPC contraction which results in surface displacement.

## References

(1)   Ebbesen, T. W.; Lezec, H. J.; Hiura, H.; Bennett, J. W.; Ghaemi, H. F.; Thio, T. Electrical Conductivity of Individual Carbon Nanotubes. *Nature* **1996**, *382* (6586), 54–56. https://doi.org/10.1038/382054a0.
(2)   Charles, A. D. M.; Rider, A. N.; Brown, S. A.; Wang, C. H. Improving the Actuation Performance of Magneto-Polymer Composites by Silane Functionalisation of Carbonyl-Iron Particles. *Compos. Part B Eng.* **2020**, *196*, 108091. https://doi.org/10.1016/j.compositesb.2020.108091.
(3)   Ryu, S. H.; Sin, J. H.; Shanmugharaj, A. M. Study on the Effect of Hexamethylene Diamine Functionalized Graphene Oxide on the Curing Kinetics of Epoxy Nanocomposites. *Eur. Polym. J.* **2014**, *52*, 88–97. https://doi.org/10.1016/j.eurpolymj.2013.12.014.